

Available online at www.sciencedirect.com



Marine Chemistry 89 (2004) 289-311



www.elsevier.com/locate/marchem

Fluorescent dissolved organic matter in marine sediment pore waters

David J. Burdige*, Scott W. Kline, Wenhao Chen¹

Department of Ocean, Earth and Atmospheric Sciences, Old Dominion University, Norfolk, VA 23529-0276, USA

Received 2 January 2003; received in revised form 26 August 2003; accepted 9 February 2004

Available online 1 June 2004

Abstract

Fluorescent dissolved organic matter (FDOM) in sediment pore waters from contrasting sites in the Chesapeake Bay and along the mid-Atlantic shelf/slope break was studied using three-dimensional fluorescence spectroscopy. Benthic fluxes of FDOM were also examined at the Chesapeake Bay sites. The major fluorescence peaks observed in these pore waters corresponded to those observed in the water column. These included peaks ascribed to the fluorescence of humic-like material (peaks A, C and M), as well as protein-like peaks that appear to result from the fluorescence of the aromatic amino acids tryptophan and tyrosine. In these pore waters we also observed a fourth humic-like fluorescence peak (A'). These four humic-like peaks appeared to occur in pairs (peaks A and M in one pair and peaks A' and C in another pair) with near identical emission maxima but different excitation maxima. Peaks A' and C were red shifted relative to peaks A and M.

Humic-like fluorescence increased with sediment depth at almost all stations, and was closely correlated with total DOC. This fluorescence appeared to be a tracer for the refractory, relatively low molecular weight pore water DOM that accumulates with depth during sediment diagenesis. Fluorescence-DOC relationships indicated that larger relative amounts of humic-like FDOM were seen in anoxic sediments versus sub-oxic or mixed redox sediments. By extension, these observations suggest that refractory humic-like compounds (in general) are preferentially preserved in sediment pore waters under anoxic conditions. A simple conceptual model is presented here which proposes that different types of organic matter (e.g., marine vs. terrestrial) as well as internal transformations of DOM or FDOM may lead to the occurrence of these humic-like fluorophores. This model is consistent with a wide range of data on FDOM in marine as well as freshwater systems. Protein-like fluorescence showed no coherent depth trends in sediment pore waters, other than the fact that pore water fluorescence intensities were greater than bottom water values. Protein-like fluorescence in pore waters may be associated with refractory DOM, although this observation is somewhat equivocal. In contrast, the results of benthic flux studies suggested that here protein-like fluorescence was associated with reactive DOM intermediates of organic matter diagenesis (e.g., dissolved peptides and proteins) produced near the sediment-water interface. Furthermore, the interplay between transport processes and the depth zonation of DOM cycling in bioirrigated sediments leads to molecular diffusion (rather than bioirrigation) playing a much more important role in transporting protein-like fluorescence out of the sediments. In contrast, bioirrigation dominates sediment-water exchange of humic-like fluorescence (and therefore most DOC in general). Finally, benthic flux studies indicated that sediments represent a source of chromophoric DOM to coastal

^{*} Corresponding author. Tel.: +1-757-683-4930.

E-mail address: dburdige@odu.edu (D.J. Burdige).

¹ Present address: Rosenstiel School of Marine and Atmospheric Science, Division of Marine and Atmospheric Chemistry, University of Miami, Miami, FL 33149-1098, USA.

waters, although further work will be needed to quantify their significance in terms of other known sources of this material (e.g., riverine input, phytoplankton degradation products).

© 2004 Elsevier B.V. All rights reserved.

Keywords: Fluorescence; Dissolved organic matter; Marine sediment pore waters

1. Introduction

The fluorescence of dissolved organic matter (DOM) is a property of the material that may reveal important information about its composition and biogeochemical cycling. Several studies have been undertaken of DOM fluorescence in marine sediment pore waters (Lyursarev et al., 1984; Chen and Bada, 1989, 1994; Chen et al., 1993; Benamou et al., 1994; De Souza Sierra et al., 1994; Coble, 1996; Skoog et al., 1996; Sierra et al., 2001; and others), although in most studies fluorescence was measured only at a single set of excitation and emission wavelengths (generally $\lambda_{\rm ex}$ =325-350 nm, $\lambda_{\rm em}$ =450 nm) thought to represent the fluorescence of dissolved humic materials. Thus, only limited information about the composition and properties of fluorescent DOM in pore waters was obtained in these studies.

In contrast, fluorescence excitation-emission matrix spectroscopy provides more detailed information about the fluorescence properties of DOM. With this technique, a three-dimensional picture is generated of fluorescence intensity as a function of excitation and emission wavelength. This technique has been applied to the study of DOM in seawater (Coble et al., 1990, 1993, 1998; Mopper and Schultz, 1993; De Souza Sierra et al., 1994, 1997; Green and Blough, 1994; Coble, 1996; Mopper et al., 1996b; Del Castillo et al., 1999; Parlanti et al., 2000; and others), and several types of DOM fluorescence have been observed with unique excitation/emission wavelength maxima (Ex_{max}/Em_{max}). The occurrence of specific fluorescence "peaks" in such 3-d fluorescence spectra, along with shifts in the position of Ex_{max}/Em_{max} values for these peaks, appear to provide some information on the composition and sources of DOM in the water column.

Studies to date have generally observed peaks associated with what has been termed humic-like fluorescence (defined as peaks A, C and M) and protein-like fluorescence (defined as peaks T and B). Protein-like fluorescence results from the fluorescence

of the aromatic amino acids tyrosine and tryptophan, either in their monomeric forms or, more likely, incorporated into reactive dissolved protein/peptides or more refractory humic-type materials (e.g., Mopper and Schultz, 1993; Mopper et al., 1996b; Mayer et al., 1999). As a result of the characteristics of the fluorescence behavior of these amino acids, differences in their observed fluorescence in natural waters may be indicative of the occurrence of proteins that are either reactive (i.e., fresh) or refractory (degraded or incorporated into humic structures; Mayer et al., 1999).

Past studies have suggested that humic-like peak M may have a marine source (Coble, 1996), while peaks A and C have been suggested as having terrestrial sources (e.g., Coble et al., 1993). It has also been proposed that peak M may simply be a blue-shifted version of peak C, implying that the fluorophore(s) responsible for peak C fluorescence is a diagenetically altered form of that responsible for peak M fluorescence (Coble, 1996; also see related discussions in Komada et al., 2002).

In this paper, we present results of 3-d fluorescence spectroscopy studies of pore waters from contrasting sites in the Chesapeake Bay and along the mid Atlantic shelf/slope break. We also examined the benthic flux of fluorescent dissolved organic matter (FDOM) from these Bay sites. The purpose of this study was to characterize FDOM in marine sediment pore waters and its flux to overlying waters. These results will allow us, in part, to examine the role of sediments as a source of FDOM to coastal waters. In addition, this fluorescence data will be used to further examine a model for DOM cycling in sediments.

2. Sample sites and methods

2.1. Sample sites

Samples were collected at two contrasting estuarine sites in Chesapeake Bay (stations M3 and S3) and at three sites along the shelf/slope break of the midAtlantic continental margin (stations AI, WC4 and WC7; see map in Burdige and Gardner, 1998). The biogeochemical characteristics of these sediments are described in detail elsewhere (e.g., Burdige et al., 2000), and will only be briefly summarized below.

Sediments at sta. M3 in the mid-Chesapeake Bay are fined-grained and sulfidic, and contain >3% total organic carbon (TOC). Sediment organic matter remineralization occurs mainly through sulfate reduction, and bioturbation appears to be insignificant. The sediments at sta. S3 in the southern Bay are silty sands with a lower TOC content ($\sim 0.5\%$). They are bioturbated and bioirrigated by large tube worms and other benthic macrofauna. These sediments have what can be considered mixed (or oscillating) oxic/anoxic sediment redox conditions (sensu Aller, 1994). Depthintegrated rates of sediment carbon oxidation (C_{ox}) are 7.2 ± 0.7 mol C m⁻² year⁻¹ at sta. M3 and 4.1 ± 1.0 mol C m⁻² year⁻¹ at sta. S3 (integrated annual averages; Burdige and Zheng, 1998).

The mid-Atlantic shelf/slope break stations (MASSB) are located approx. 100 miles southeast of the mouth of Delaware Bay at water depths of $\sim 400-750$ m. The sediments here are grey/green silty clays and contain $\sim 2\%$ TOC. Some bioturbation $(D_{\rm B}\approx 1.5-5.0~{\rm cm^2/year})$ occurs in the upper 20–30 cm of these sediments (Ferdelman, 1994). Pore water profiles suggest that sub-oxic remineralization dominates the upper 20–30 cm of these sediments (Burdige, unpublished data). Linear sulfate gradients $(\Delta [{\rm SO_4^2}]\approx 1~{\rm mM}~{\rm over}~25~{\rm cm})$ also imply that anoxic remineralization (sulfate reduction) occurs at depth in these sediments. Average $C_{\rm ox}$ values at the three MASSB sites range from 0.7 to 1.7 mol C m $^{-2}$ year $^{-1}$ (Burdige et al., 2000).

2.2. Pore water collection

All sediments were collected by box core and subcored for further sampling. Sub-cores at sta. M3 and the MASSB sites were processed under N₂ and pore waters were obtained by centrifugation (Burdige and Zheng, 1998). Pore waters were extracted from sta. S3 sediments without exposure to air using a modified pressurized core barrel technique (Burdige and Gardner, 1998). This procedure was used to avoid possible artifacts associated with collection by centrifugation of pore water samples for DOM analyses from heavily

bioturbated sediments (Martin and McCorkle, 1993; Alperin et al., 1999). Regardless of the method of sample collection, all samples were filtered through 0.45 μm Gelman Nylon Acrodisc filters and stored frozen (-20 °C) in amber glass vials until analyzed.

2.3. Benthic flux studies and diffusive flux calculations

Sediment cores used for benthic flux studies at Chesapeake Bay sta. S3 and M3 were collected in 11/97 (cruise CH XX) as described above. Benthic fluxes were determined with these cores using incubation techniques described in detail in Burdige and Zheng (1998).

Using pore water data from parallel cores collected on this date, diffusive fluxes of DOC and FDOM from these sediments were calculated as done previously (Burdige et al., 1999b) using Fick's first law of diffusion $(J=-\varphi_0D_s dC/dz_0)$. In this calculation we assumed that the DOC and FDOM concentration gradients across the sediment-water interface (dC/ dz_0) could be approximated by $\Delta C/\Delta z$, where ΔC is the concentration difference between the bottom waters and the first sediment sample, and Δz is the depth of the midpoint of this sediment sample (e.g., 0.25 cm for a 0-0.5 cm sediment sample). The free solution diffusion coefficient (D°) for DOC and FDOM used here was 0.157 ± 0.065 cm²/day, based on: the assumption that the average molecular weight of pore water DOM is between 1 and 10 kDa (Burdige and Gardner, 1998); an observed inverse cube root relationship between molecular weight and the free solution diffusion coefficient (D°) for an organic compound (Burdige et al., 1992; Alperin et al., 1994); a bottom water temperature of 15 °C at the time of core collection. This value of D° was corrected for sediment tortuosity and converted to a bulk sediment diffusion coefficient (D_s) as described in Burdige et al. (1999b).

2.4. Fluorescence measurements

All the samples were analyzed using a Spex Industries FluoroMax-2 spectrofluorometer, with scans controlled by DataMax spectroscopy software. Three dimensional excitation—emission fluorescence spectra were obtained by collecting individual emis-

sion spectra (290-560 nm) over a range of excitation wavelengths (200-440 nm), and then merging the data together into a single three-dimensional multifile. The scan increments for excitation and emission wavelengths were 5 and 2 nm, respectively, and the data integration time was 0.1 s. Data acquisition was carried out in the S/R (signal/reference) mode, which normalizes the fluorescence emission signal with the intensity of the excitation light, and thus accounts for variations in the intensity of the excitation lamp over the excitation wavelengths used. A long pass filter (Corion, CG-431-01, wavelength cut-off: 290 nm) was placed in the emission light path to remove signals from second order Rayleigh and Raman scattering. Signals from first order Rayleigh scattering were removed from emission spectra by instrumental software.

Samples such as the ones we examined here are highly fluorescent, and can be subject to inner filter effects during analysis. These effects are caused by the absorption of either the initial excitation light or the light emitted by the fluorophore, by components of the solution matrix (Harris and Bashford, 1987). Inner filter effects can therefore be a major cause for a non-linear relationship between fluorescence intensity and concentration. Dilution of the sample usually reduces the overall light absorption of the solution and in most cases the expected linear relationship between fluorescence intensity and concentration, as derived from the Beer-Lambert Law, is then observed. Harris and Bashford (1987) suggest that to preserve this linearity the overall absorbance (a) of a sample at a given excitation wavelength should not exceed 0.05 cm⁻¹. For these reasons, we developed the following procedure to analyze our samples. Fluorescence spectra and UV-Vis absorption spectra (200-800 nm) were initially obtained with undiluted samples to provide us with initial information on peak locations, to determine the necessary sample dilutions for later analyses of these samples, and to provide a check for contamination of diluted samples. Samples with absorbance values exceeding 0.05 cm⁻¹ at 220 nm (the lowest excitation wavelength of peaks observed in this study) were then diluted accordingly with UV photooxidized seawater of similar salinity, and then reanalyzed for fluorescence and absorbance. Inner filter effects in undiluted samples can also be corrected mathematically (Holland et al., 1977; Yappert and Ingle, 1989; Tucker et al., 1992), and in selected samples we compared fluorescence values in diluted and undiluted samples as an internal check for contamination during sample processing (dilution).

All post-collection data manipulation was performed using Grams/32 software (Galactic Industries). Raw fluorescence files were corrected for wavelengthdependent instrumental variation in both the excitation (200-600 nm) and emission (290-750 nm) directions. Excitation correction factors were created utilizing a solution of Rhodamine B in1,2-dipropanol as the quantum counter (Lakowicz, 1999). Emission correction factors were provided by Spex Industries and were created utilizing a standard Xenon lamp source, as described by Lakowicz (1999). Instrumentcorrected spectra were then blank corrected using a 3d fluorescence spectrum of UV photo-oxidized seawater of similar salinity to the sample, which was run each day of measurements. Instrument- and blankcorrected spectra were then interpolated (4 point spline) four times in the excitation direction and two times in the emission direction and smoothed utilizing a 25-point Savitsky-Golay routine.

The positions and intensities of individual fluorescence peaks (determined by their Ex_{max}/Em_{max} values) were determined by visually examining these corrected 3-d fluorescence spectra. These intensities were converted to units of ppb quinine sulfate using the slope of a quinine sulfate standard curve, which was run daily using the constant wavelength acquisition mode (λ_{excit} =350 nm, λ_{emiss} =450 nm). Standards used here ranged from 1 to 50 ppb quinine sulfate dihydrate (Fluka, Switzerland, cat. no. GA11338) in 0.1 N sulfuric acid. The normalization of fluorescence intensities to quinine sulfate fluorescence converts all of our measured fluorescence values to a constant set of units (ppb QS), and factors outs day-to-day fluctuations (e.g., lamp intensity) in the operation of the spectrofluorometer. This approach also allows our results to be more easily compared with fluorescence measurements made by other workers that are similarly calibrated to this (or any other independent) standard. While this approach gives one quantitative information about the magnitude of the fluorescence from a particular type of fluorophore (e.g., humic-like vs. protein-like) it is also important to remember that little is known about the specific compounds responsible for the observed fluorescence signals, and their quantum yields or the number of fluorophores per mole carbon (or per mole FDOM "compound"). Thus, the use of this fluorescence data in certain types of comparisons is limited.

2.5. Additional measurements

Dissolved organic carbon (DOC) was determined by high temperature catalytic oxidation methods (Burdige and Gardner, 1998). Absorption spectra (UV-VIS) of selected samples were determined with a Hewlett Packard 8453 UV-Visible spectrometer in a 1-cm quartz cuvette. Spectra were recorded from 200-800 nm, and measured absorbances (A) were converted to absorption coefficients with the equation $a(\lambda)=2.303A(\lambda)/r$, where r is the cell path length. Absorption spectra from most natural waters generally show a simple exponential-like decrease with increasing wavelength (e.g., Blough and Green, 1995), and we therefore fit our data to the commonly used equation, $a(\lambda)=a(\lambda)e^{-S(\lambda-\lambda o)}$. In this equation λ_o was taken to be 290 nm, and S (also referred to as the spectral slope) is a quantitative indication of how rapidly a given absorption spectrum attenuates with increasing wavelength. In fitting the data we first used the average absorption coefficient from 700 to 800 nm to correct the spectra for refractive index effects (Green and Blough, 1994). Using corrected absorption data from 290 to 450 nm we then fit $\ln a(\lambda)$ versus λ by linear-least-squares fitting. Based on this latter equation the slope of the best-fit line through this natural log-transformed data is S (see Mopper et al., 1996a for further details).

3. Results

3.1. Fluorescence properties of pore water DOM

Fluorescence spectra such as those we have obtained contain a number of distinct peaks that are generally ascribed to either humic-like or protein-like fluorescence (see Fig. 1). As in other studies, peaks were identified based on observed fluorescence maxima in three-dimensional plots of fluorescence intensity versus excitation and emission wavelength (note that while Fig. 1 shows two-dimensional contour plots, such 3-d plots can be seen in, e.g., Coble,

1996, or Coble et al., 1998). The excitation and emission wavelengths of the major fluorescence peaks observed in this study are listed in Table 1.

In some cases, the overlap of neighboring peaks led to one peak appearing as a shoulder on the tail of a larger adjacent peak. This often occurred because of the overlap of a broad humic-like peak with a narrower protein-like peak. As discussed in Matthews et al. (1996) the deconvolution of such complex spectra is more complicated than that described above. In their examination of this problem, Matthews et al. (1996) attempted to simulate the observed 3-d fluorescence spectrum of a coral extract with a series of Gaussian elliptical peak. The resulting synthetic peaks that best characterized the original spectra agreed reasonably well with peaks seen in the actual spectra, and had Exmax and Emmax values that were very similar to those we observed (Table 1). Furthermore, calculations we have done (by mathematically adding together two Gaussian peaks over a range of peak widths and peak separations) also support these observations. These calculations suggest that spectral shifts in Exmax or Emmax values in such additive spectra as a result of peak overlap (as compared to values in the initial individual spectra) are ~10 nm or less, and therefore are within the range of uncertainties for Exmax or Emmax values listed in Table 1. At the same time, intensities of the individual peaks in such additive spectra (as compared to those in the initial individual spectra) are virtually unchanged for broad peaks, and increase by less than $\sim 40\%$ for narrow (i.e., protein-like) peaks that fall on the shoulder of a broad (i.e., humic-like) peak. Therefore, while more sophisticated peak deconvolution techniques (such as those described by Matthews et al., 1996) would provide somewhat better resolution of the peaks in our spectra, the observations discussed here also suggest that our approach is sufficient for quantifying fluorescence peaks in our pore waters.

Past studies have reported two protein-like fluorescence peaks: peak B ($\rm Ex_{max}$ =270–280 nm, $\rm Em_{max}$ =300–305 nm) due to tyrosine (tyr) fluorescence, and peak T ($\rm Ex_{max}$ =270–280 nm, $\rm Em_{max}$ =340–350 nm) due to tryptophan (try) fluorescence (e.g., Coble, 1996; Lakowicz, 1999). Based on the examination of fluorescence spectra for individual amino acid solutions and a solution of the protein bovine serum

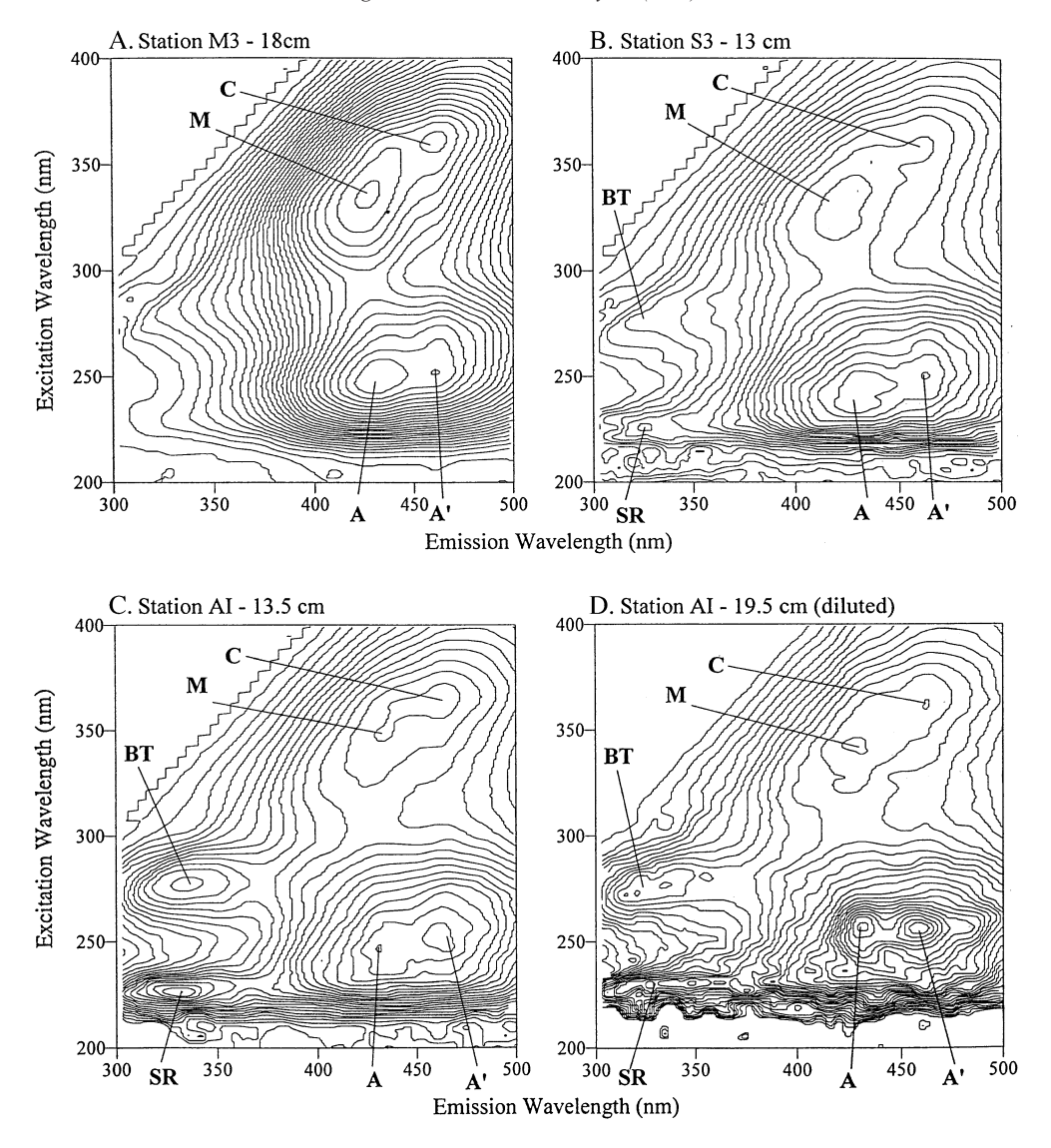


Fig. 1. Representative EEMS contour plots for pore water samples from sta. M3 (11/97) and S3 (11/97) in the Chesapeake Bay and sta. AI (6/97) on the mid-Atlantic shelf/slope break. Spectra A–C are for undiluted pore water samples while spectrum D is for a sample that was diluted approximately 1:5 with UV-oxidized seawater (see Section 2.4 for further details). Note the occurrence of apparent humic-like fluorescence peak pairs (peaks A and M and peaks A' and C) with near identical Em_{max} values and different Ex_{max} values. Contour intervals in each spectrum (ppb QS/contour line) were: (A) 11.05; (B) 2.29; (C) 2.01; (D) 0.81. The maximum fluorescence in each spectrum (ppb QS) was: (A) 809 (peak A); (B) 92 (peak A'); (D) 92 (peak A').

albumin (BSA), we have also confirmed the existence of two additional protein-like fluorescence peaks at lower excitation wavelengths (Ex_{max}=220–230 nm) and similar emission wavelengths (see published spectra in Mayer et al., 1999, that are similar to those we have observed). These are a tryptophan peak which we call peak R and a tyrosine

peak which we call peak S. These low excitation wavelengths protein-like peaks have generally not been seen in other studies because these studies typically did not use excitation wavelengths that were low enough to detect this type of fluorescence (see Mopper and Schultz, 1993, as an exception to this general observation).

Table 1 Fluorescence peaks observed in the sediment pore waters of this study

Peak	Ex _{max} (nm)	Em _{max} (nm)	
Humic-like	e fluorescence		
A	$239\pm10 \ (220-257)$	$429\pm4~(419-438)$	
M	$328\pm10 \ (302-357)$	422 ± 6 (410-436)	
A'	248 ± 9 (224-261)	461±4 (449-466)	
C	$360\pm4\ (348-369)$	460±3 (450-467)	
Protein-lik	e fluorescence		
SR	$224\pm4~(220-250)$	$324\pm8 (304-345)$	
BT	274 ± 2 (268-279)	$324\pm8 (306-339)$	

The values in parentheses are the observed ranges in our data set for the excitation and emission wavelengths for each peak. Although some of the ranges shown in this table can be quite large (up to 50 nm), this is generally due to one or two "flyers" in the data sets, as can be seen in the relatively small standard deviations (less than 10 nm) of the average $\rm Ex_{max}$ and $\rm Em_{max}$ values for each peak.

In our initial work identifying protein-like fluorescence peaks in our spectra, we attempted to differentiate between tyr and try peaks at high and low Ex_{max} values (e.g., peaks B and T at $\sim 270-280$ nm and peaks S and R at $\sim 220-230$ nm). However, a variety of practical considerations (e.g., spectral interferences such as those discussed above), as well as the complexity of the fluorescence response of these amino acids when combined in proteins and peptides (e.g., see discussions in Mayer et al., 1999; Lakowicz, 1999) made such differentiation between tyr and try peaks (at a given Ex_{max} value) equivocal at best. Therefore, here we have chosen to simply quantify protein-like fluorescence in terms of high and low energy excitation "peaks" (i.e., combined peaks BT and SR) without any specific indication of the potential amino acid source of the fluorescence (e.g., see Table 1).

Humic-like fluorescence peaks A, C and M occurred at $\rm Em_{max}$ and $\rm Ex_{max}$ values that were similar to those observed in previous studies (see references in Section 1). In assigning names to peaks in our spectra, we made the assumption that peak M was a distinct peak blue-shifted relative to peak C and for humic-like peaks with $\rm Ex_{max}$ values greater than 300 nm we used an emission wavelength cut-off of 440 nm to differentiate between these two peaks.

In our work we have also detected a previously unreported peak that we have designated peak A' (see Fig. 1). In conjunction with the other three humic-like

fluorescence peaks (A, C, and M) these four peaks appeared to exist in pairs (peaks A and M and peaks A' and C) with near-identical Em_{max} values and different Ex_{max} values for each pair. This peak pairing shows some similarity to emission bands often observed in 3-d fluorescence spectra for single chromophore systems, such as that seen with peaks T and R for tryptophan fluorescence and peaks B and S seen for tyrosine fluorescence (e.g., see discussions in Blough and Green, 1995).

An examination of the $\rm Ex_{max}$ and $\rm Em_{max}$ values in Table 1 indicated that there was little variation in these values in the pore waters we studied. At a given site there also did not appear to be consistent depth trends in $\rm Ex_{max}$ and $\rm Em_{max}$ values (results not plotted here), nor did there appear to be any significant differences in these values in estuarine versus shelf/slope break sediment pore waters.

The peak intensity ratios for the humic-like peaks were constant across these differing sites (Table 2) as well as with depth at a given site (results not plotted here). Similar constancy was also seen for protein-like fluorescence peak ratios. Within their uncertainty these protein-like peak ratios in pore waters (\sim 2) were similar to those observed in authentic amino acids standards or in the protein BSA (results not shown here).

3.2. Distribution of pore water fluorescence

Given the constancy of the peak ratios for humic-like fluorescence in these pore waters, we have chosen to simply plot depth distributions of peak M humic-like fluorescence for the five sites we studied (Fig. 2). The shapes of the depth profiles for any of the other humic-like peaks will then be similar to those shown here, scaled by the ratios in Table 2.

Table 2 Humic and protein-like peak ratios

Training and protein mic pean ratios				
Region	A/M	A'/C	M/C	
Chesapeake Bay Shelf/slope Break	2.1 ± 0.3 1.9 ± 0.4	2.1 ± 0.2 1.8 ± 0.3	1.1 ± 0.1 1.0 ± 0.1	(n=49) ^a (n=46) ^a
	SR/BT			
Chesapeake Bay Shelf/slope break	2.3±0.6 1.8±0.6	(n=33) (n=48)		

^a For all three peak ratios.

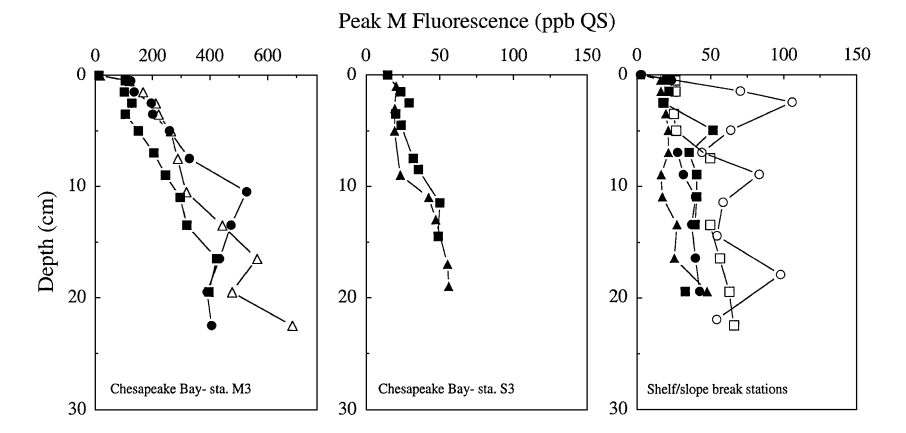


Fig. 2. Pore water depth profiles of the intensity of humic-like peak M. (left panel) Cores collected at mid-Chesapeake Bay sta. M3 in 8/96 (cruise CH XVII; △), 8/97 (cruise CH XIX; ●), and 11/97 (cruise CH XX; ■). (center panel) Cores collected at southern Chesapeake Bay sta. S3 in 8/97 (cruise CH XIX; ■) and 11/97 (cruise CH XX; ▲). (right panel) Cores collected at shelf/slope break sta. AI in 8/96 (cruise CH XVII; ○) and 8/97 (cruise CH XIX; ●); sta. WC7 in 8/96 (CH XVII; □) and in 8/97 (CH XIX; ■); and at sta. WC4 in 8/97 (CH XIX; ▲).

In sta. M3 pore waters humic-like fluorescence increased with depth, and depth profiles on different sampling dates did not show significant differences. These pore waters were extremely fluorescent, with pore water fluorescence values over an order of magnitude higher than that seen in the bottom waters. In contrast, at sta. S3 humic-like fluorescence was much weaker than that at sta. M3, and only increased by a factor of ~2 over the upper 20 cm of sediment. At the MASSB stations (AI, WC4 and WC7), humic-like fluorescence depth profiles were similar to one another, with pore water gradients more similar to sta. S3 than to M3.

Depth profiles of protein-like fluorescence peak BT are shown in Fig. 3. As was the case for humiclike fluorescence, depth profiles of peak SR fluorescence will have a similar shape as these profiles, again scaled by the ratio in Table 2. An examination of these results indicates that protein-like fluorescence was generally higher at sta. M3, with values at sta. S3 and the MASSB stations again being more similar in magnitude. Like humic-like fluorescence, protein-like fluorescence was generally higher in pore waters than in bottom waters. At sta. M3 there may also be a slight increase with depth in both types of protein-like fluorescence. However at the other stations there appeared to be little coherent depth structure in these pore water profiles beyond an overall increase in pore water values relative to bottom water values.

3.3. Fluorescence–DOC relationships

Concentrations of DOC increase with depth in these sediments, often times in an exponential-like fashion (see the DOC profiles for many of the cores discussed here in Burdige and Gardner, 1998; Burdige and Zheng, 1998; Burdige et al., 2000). The shapes of these profiles are similar to those seen here for pore water humic-like fluorescence. Profiles of

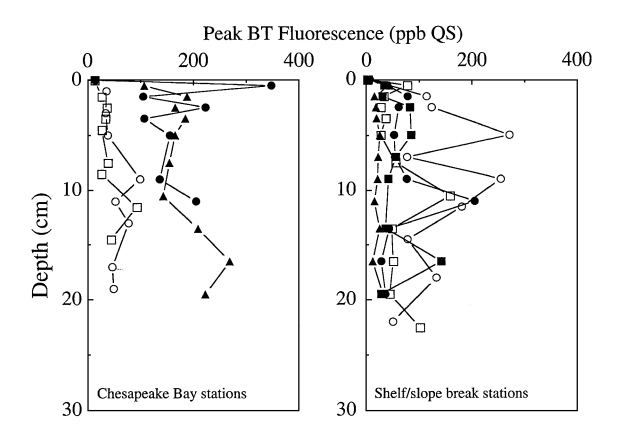


Fig. 3. Pore water depth profiles of the intensity of protein-like peak BT. (left panel) Cores collected at mid-Chesapeake Bay sta. M3 in 8/96 (cruise CH XVII; ▲) and 8/97 (cruise CH XIX; ●), and cores collected at southern Chesapeake Bay sta. S3 in 8/97 (cruise CH XIX; □) and 11/97 (cruise CH XX; ○). (right panel) Cores collected at shelf/slope break sta. AI in 8/96 (cruise CH XVII; ○) and 8/97 (cruise CH XIX; ●), sta. WC7 in 8/96 (CH XVII; □) and in 8/97 (CH XIX; ■), and sta. WC4 in 8/97 (CH XIX; ▲).

pore water peak M fluorescence intensities normalized to DOC concentrations are shown in Fig. 4 (again similar plots for other humic-like peaks would have the same shapes and would be scaled by the ratios shown in Table 2). In general, normalized pore water fluorescence values were higher than bottom water values and with the exception of perhaps sta. S3, showed no significant increase with sediment depth. These ratios were also higher in sta. M3 Chesapeake Bay sediments (>200 ppb QS/mM) than they were in the sta. S3 or MASSB sediments (generally 50–100 ppb QS/mM).

Another way to view this data involves using property–property plots of pore water DOM fluorescence versus DOC concentrations. Such plots for humic-like fluorescence are shown in Fig. 5 for peaks A and M, and the best-fit values for the property–property plots for all humic-like peaks are listed in Table 3. As these results indicate, there appear to be separate and distinct trend lines for the Chesapeake Bay (estuarine) and the MASSB (off-shore) sediment pore waters. These relationships are highly significant (p<0.01 for all but one peak/site pair) and for the most part the slopes of these lines are consistent with the values in the depth plots in Fig. 4. They demonstrate that on a per mole carbon basis, DOM from these

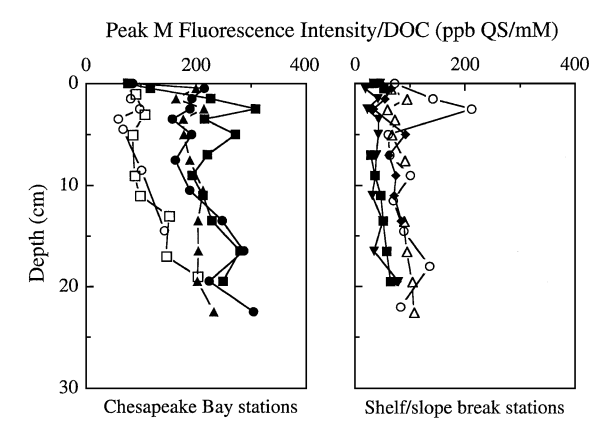


Fig. 4. Depth profiles of pore water peak M humic-like fluorescence intensity normalized to DOC concentrations. (left panel) Cores collected at mid-Chesapeake Bay sta. M3 in 8/96 (cruise CH XVII; ▲), 8/97 (cruise CH XIX; ●), and 11/97 (cruise CH XX: ■), and at southern Chesapeake Bay sta. S3 in 8/97 (cruise CH XIX; ○) and 11/97 (cruise CH XX; □). (right panel) Cores collected at shelf/slope break sta. AI in 8/96 (cruise CH XVII; ○) and 8/97 (cruise CH XIX; ●), sta. WC7 in 8/96 (CH XVII; □) and in 8/97 (CH XIX; ■), and sta. WC4 in 8/97 (CH XIX; ▲).

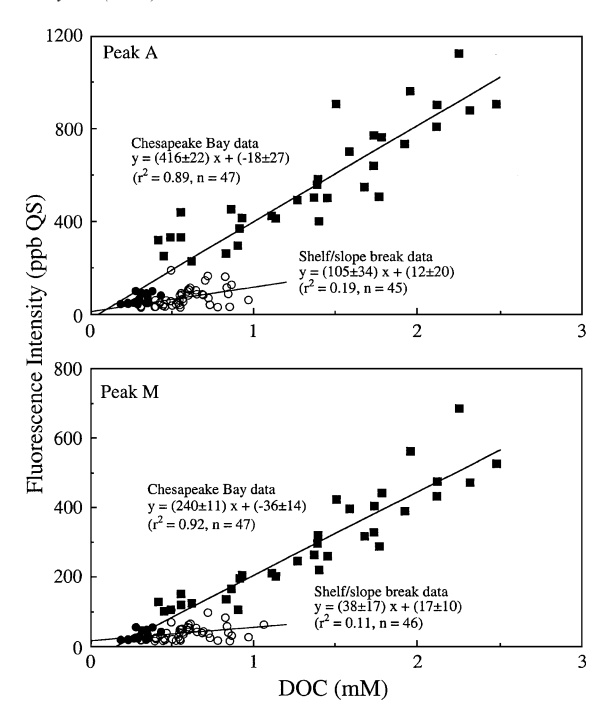


Fig. 5. Peaks A and M fluorescence intensity versus DOC concentration in Chesapeake Bay and shelf/slope break sediment pore waters. Also shown here are the best-fit lines through each of the data sets. Symbols: Chesapeake Bay, sta. M3 (■; data from CHXVII, CH XIX and CH XX); Chesapeake Bay, sta. S3 (●; data from CH XIX and CH XX); MASSB stations (O; data from sta. AI CH XVII and XIX, sta. WC7 CH XVII and XIX, and sta. WC4 CH XIX).

estuarine sediment pore waters is more fluorescent than that from these continental margin sediments.

Although we have chosen here to fit the sta. S3 data along with the sta. M3 data (Fig. 5), the sta. S3 fluorescence:DOC ratios shown in Fig. 4 are actually more similar to values seen in MASSB sediments. This result is perhaps not surprising since the slopes of the Chesapeake Bay plots shown in Fig. 5 are mainly controlled by the sta. M3 data, hence the similarity between the slopes of these lines and the fluorescence to DOC ratios for sta. M3 sediments shown in Fig. 4. Furthermore, a careful examination of Fig. 5 indicates that the sta. S3 data fall in the cross-over region between the two best-fit lines, and in fact may actually "belong" on the shelf/slope break line (consistent with the results in Fig. 4). The significance of this latter observation will be discussed in further detail in Section 4.5.

Table 3
Summary of fluorescence/DOC relationships^a

	Peak A ^b	Peak C ^b	Peak A'	Peak M
Chesapeake bay				
slope (ppb QS/mM) r ² ANOVA ^b n	416±22 0.89 <i>p</i> <0.001 47	205±9 0.92 <i>p</i> <0.001 45	375±15 0.94 <i>p</i> <0.001 45	240 ± 11 0.92 $p<0.001$ 47
Shelf/slope break				
slope (ppb QS/mM) r^2	105 ± 34 0.19	63 ± 16 0.24	88 ± 27 0.20	38 ± 17 0.11
ANOVA ^c	<i>p</i> <0.01 45	<i>p</i> <0.001 49	<i>p</i> <0.002	<i>p</i> <0.05

^a All of these fluorescence–DOC relationships have small, non-zero y-intercepts, although the values are all indistinguishable from zero and are therefore not listed here.

Protein-like fluorescence was also positively correlated with DOC concentrations (Fig. 6), with both correlations being significant (p<0.01). In contrast however with humic-like fluorescence, there did not appear to be the same intra-site differences between correlations of protein-like fluorescence and DOC concentrations (compare Figs. 5 and 6).

3.4. UV-Vis absorbance and fluorescence/absorbance ratios

Average S values were slightly higher in Chesapeake Bay pore waters $(16.8\pm3.1\times10^3 \text{ nm}^{-1})$ than they were in shelf/slope break sediment pore waters $(13.0\pm2.2\times10^3 \text{ nm}^{-1})$. Chesapeake Bay sediment pore water S values showed no significant depth variations in the sediments and were slightly lower than bottom water values ($\sim 20 \times 10^3 \text{ nm}^{-1}$; results not plotted here). Shelf/slope break pore waters showed no apparent gradient with sediment depth or across the sediment-water interface. The spectral slopes reported here are within the range of S values observed by Seretti et al. (1997) for pore waters from Adriatic Sea sediments. They are also intermediate between S values observed for terrestrial humic acids (that can be as low as $\sim 10 \times 10^3 \text{ nm}^{-1}$) and open ocean CDOM ($S \approx 20-30 \times 10^3 \text{ nm}^{-1}$), and are similar to reported values for coastal waters

influenced by riverine inputs (Blough and Green, 1995).

For a given fluorescence peak, its fluorescence: absorbance ratio (i.e., the fluorescence intensity of the peak divided by the measured absorption at the peak Ex_{max} value) is an indicator of the apparent fluorescence efficiency or DOM fluorescence quantum yield (Green and Blough, 1994; Mopper et al., 1996a). For the four humic-like peaks, this ratio showed no significant differences among sites or with depth at a given site (results not shown here).

3.5. Benthic fluxes of DOC and FDOM

The results of benthic flux studies carried out at Chesapeake Bay sta. S3 and M3 with cores collected in 11/97 are listed in Table 4. The benthic DOC fluxes reported here are similar to previous values determined at these sites (see Burdige, 2001 for a recent summary). Fluxes of humic-like FDOM (peaks C and M fluorescence) agreed well with FDOM fluxes determined by Skoog et al. (1996) in seasonal studies in the sediments of Gullmar Fjord, Sweden (their range: -3 to $\sim 170~\mu g$ QS m⁻² day⁻¹). However, we also note that this comparison is not entirely straightforward since Skoog et al. (1996) examined fluorescence at λ_{ex} =350 nm and λ_{em} =450 nm, and

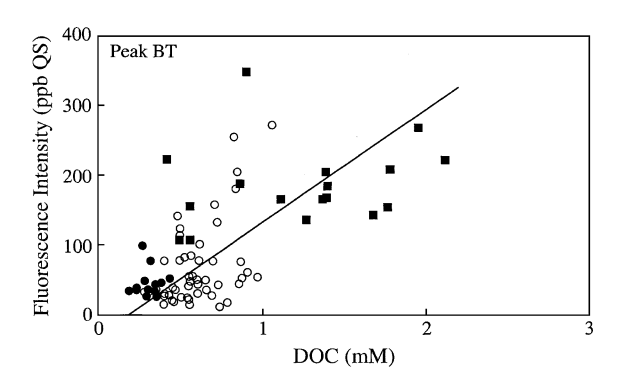


Fig. 6. Peak BT fluorescence intensity versus DOC concentrations in Chesapeake Bay and shelf/slope break sediment pore waters. Also shown here are the best-fit lines through each of the data sets. Symbols: Chesapeake Bay, sta. M3 (■; data from CHXVII and CHXIX); Chesapeake Bay, sta. S3 (●; data from CHXIX and CHXX); MASSB stations (O; data sta. AI CHXVII and XIX, sta. WC7 XVII and XIX, and sta. WC4 XIX). Note that similar trends are seen in a plot of peak SR fluorescence intensity versus DOC concentrations in these pore waters.

^b See Fig. 5.

^c Analysis of variance results indicating the probability that the observed relationship between fluorescence and DOC occurred simply by chance.

Table 4
Results from Chesapeake bay benthic flux studies

		sta. M3	sta. S3	M3/S3 ^a
DOC	(Measured) ^b	1.10 ± 0.36	0.27 ± 0.05	4.1±1.9
	(Calculated) ^{b,c}	0.96 ± 0.40	0.02 ± 0.01	
Peak A	(Measured) ^b	314 ± 144	62 ± 6	5.1 ± 2.4
	(Calculated) ^{b,c}	484 ± 202	13 ± 5	
Peak M	(Measured) ^b	166 ± 68	43 ± 4	3.9 ± 1.6
	(Calculated) ^{b,c}	254 ± 106	5 ± 2	
Peak A'	(Measured) ^b	328 ± 151	55 ± 7	6.0 ± 2.9
	(Calculated) ^{b,c}	484 ± 202	13 ± 6	
Peak C	(Measured) ^b	171 ± 89	45 ± 3	3.8 ± 2.0
	(Calculated) ^{b,c}	218 ± 91	5 ± 2	
Peak BT	(Measured) ^b	89 ± 41	39 ± 11	2.3 ± 1.7
	(Calculated) ^{b,c}	390 ± 163	12 ± 5	
Peak SR	(Measured) ^b	112 ± 48	53 ± 149	2.1 ± 6
	(Calculated) ^{b,c}	nc ^d	35 ± 15	
Humic peaks				4.7 ± 2.3
Protein peaks				2.2 ± 3.1
C _{ox} ^e		31.3 ± 9.0	4.8 ± 1.0	6.6 ± 2.3
Protein/Humic ^f		~ 0.4	~ 0.9	
Peak A/DOC ^g		282 ± 157	228 ± 46	
Peak M/DOC ^g		149 ± 77	158 ± 31	
Peak A'/DOC ^g		294 ± 164	200 ± 44	
Peak C/DOC ^g		154 ± 94	165 ± 31	

^a The ratio of measured fluxes at station M3 to those at station S3.

based on the results in Table 1, this DOM fluorescence falls in-between the $\rm Ex_{max}/\rm Em_{max}$ values for these two humic-like peaks.

At both sites, fluxes of humic-like FDOM were generally greater than fluxes of protein-like FDOM, although the difference was greater at sta. S3 than it was a sta. M3 (Table 4). The ratios of FDOM fluxes at stations M3 versus S3 were essentially identical to that for total DOC (4.7 ± 2.3 versus 4.1 ± 1.9), and were similar to the same ratio for C_{ox} values (6.6 ± 2.3). These ratios for protein-like fluorescence,

however, may have been lower (2.2 ± 3.1) . Measured benthic fluxes and calculated, diffusive fluxes of DOC and humic-like FDOM were essentially identical at sta. M3 ($R\approx1$ in Fig. 7), while at sta. S3 measured benthic fluxes of total DOC and humic-like FDOM were significantly larger than calculated, diffusive fluxes ($R\approx8-10$). In contrast, at sta. S3 measured benthic fluxes and calculated, diffusive fluxes of protein-like FDOM appeared to be more similar to one another ($R\approx2$).

Although it is difficult to quantify it as a benthic flux, *S* values in the waters overlying benthic flux cores decreased with time during benthic flux determinations (data not shown here). These results demonstrate that the CDOM effluxing out of these sediments had *S* values that were lower than bottom water values, consistent with the *S* value pore water gradients in Chesapeake Bay sediments discussed in Section 3.4.

4. Discussion

4.1. Humic-like fluorescence of pore water DOM—general considerations

As noted above, past studies of DOM fluorescence have observed many of the protein-like and humic-like fluorescence peaks we observed in these sediment pore waters. At the same time, other workers have reported peaks in 3-d fluorescence spectra that we do not see evidence for in these pore waters.

Matthews et al. (1996) discuss a low energy peak with an Ex_{max}/Em_{max} of 480/540 nm that is typical of terrestrial (lignin-derived) humic acids. Since our fluorescence scans end at excitation wavelengths of 440 nm, we are unable to state definitively that this peak is not observed in our samples. However, in our spectra we see no evidence for the tail of this peak in the upper ends of our spectra. Thus, either this peak is not found in our samples or it is relatively small and obscured by the large tail of peak C. Coble et al. (1998) observed a peak N in Arabian Sea waters with an Ex_{max}/Em_{max} of 280/370 nm, which they argue is associated with biological activity in surface ocean waters. Again, in our pore waters we see no evidence of this peak.

More importantly though, in our samples we have observed a new humic-like peak, peak A'. Along with

^b DOC fluxes are in units of mmol/ m^2 /day. Fluxes of fluorescent material are $\mu g \, QS/m^2$ /day. Positive fluxes are out of the sediments.

^c Diffusive fluxes were calculated as discussed in the text.

^d Not calculated due to a lack of detectable peaks in pore water samples.

 $^{^{\}rm c}$ $C_{\rm ox}$ is the depth-integrated rate of sediment carbon oxidation determined with ΣCO_2 benthic flux measurements (see Burdige and Zheng, 1998, for further details).

^f The range of measured benthic fluxes of protein-like FDOM over humic-like FDOM, based on averages of the high energy (A, A', and SR) and low energy (M, C, and BT) humic-like and protein-like FDOM peaks.

 $^{^{}g}$ Units of μg QS/mmol DOC (equivalent to ppbQS/mM DOC, the units used to express DOC-normalized pore water fluorescence values).

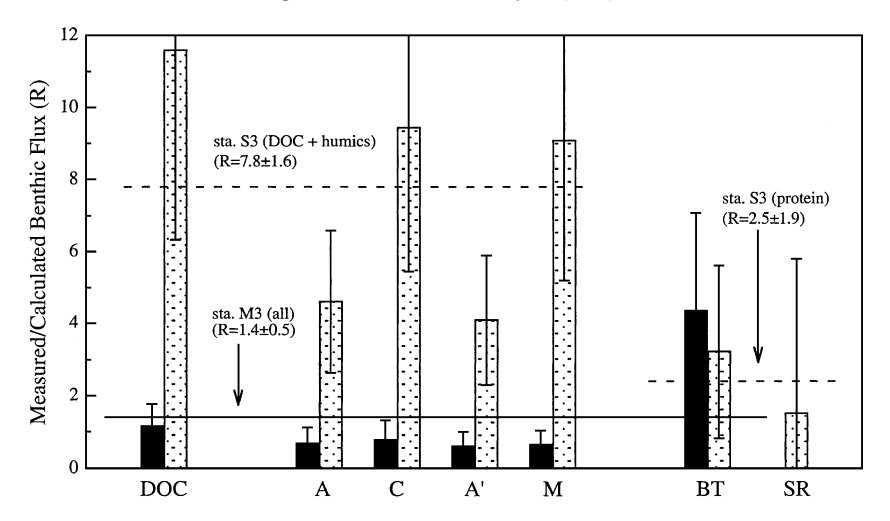


Fig. 7. The ratio of measured to calculated, diffusive benthic fluxes of DOC, humic-like FDOM (peaks A, C, A' and M) and protein-like FDOM (peaks BT and SR). Measured benthic fluxes are listed in Table 4 and calculated, diffusive fluxes were determined as discussed in the text. Station M3 results are black bars and sta. S3 results are stippled bars. The absence of a bar for protein-like peak SR at sta. M3 is due to our inability to detect this peak in pore water samples at this site on this sampling date. Also shown here are average R values for all sta. M3 benthic fluxes and for sta. S3, separated into two groups (DOC+humic-like fluorescence benthic fluxes and protein-like fluorescence benthic fluxes).

previously observed humic-like peaks A, C, and M, these four peaks appeared to occur in pairs that had near-identical Em_{max} values and different Ex_{max} values (see Table 1). With the caveats discussed below we refer to these peak pairs as "apparent" emission bands, since their behavior has some degree of similarity to that seen in emission bands for simple single chromophore systems. By making this analogy though, we do not wish to suggest that there are simply two different fluorophores responsible for humic-like DOM fluorescence, since neither our data (nor any other data in the literature) would support this suggestion. Results in Boehme and Coble (2000) further show that this is not the case (see the discussion below for further details). Rather, we believe that these apparent peak pairs may represent two broad classes of fluorophores, each of which is composed of some unknown group of individual fluorophores with similar fluorescence properties. Furthermore, the sources and diagenetic behavior of each of these two groups of fluorophores are also likely sufficiently linked (also see Section 4.2) such that in 3-d fluorescence spectra these peak pairs show this broad similarity to emission bands seen in simple chromophores.

This description of humic-like fluorescence is consistent with a model presented by De Souza Sierra

et al. (1994) for humic-like fluorescence. Using single wavelength excitation (λ_{ob} =445 nm) and emission ($\lambda_{\rm ex}$ =250, 313 and 370 nm) spectra and synchronous scan excitation-emission spectra, they proposed a model in which humic-like fluorescence could be explained by two chromophore classes (termed α and B) that occur in apparent emission bands that are similar to those discussed here. Based on the proposed properties of these fluorophores our results are consistent with this model if one assumes that chromophore class α leads to fluorescence peaks A' and C, and that chromophore class β leads to fluorescence peaks A and M (see Table 5). De Souza Sierra et al. (1994) also argue that the β-type chromophores are likely of marine origin while the α -type chromophores may be terrestrially derived (also see Sierra et al., 2001). The significance of this suggestion will be discussed below.

An examination of Table 5 indicates that there is not an exact correspondence between the maximum excitation and emission wavelengths for the proposed α and β chromophore classes and the Ex_{max} and Em_{max} for fluorescence peaks A, A', C and M (Table 1). This most likely occurs because defining the fluorescence properties of these proposed chromophore classes is constrained by the limited number of excitation and emission spectra used in the study by

Table 5 A comparison of the properties of the α and β chromophores described by De Souza Sierra et al. (1994) with the fluorescence peaks observed in this study

Excitation or emission band ^a	Excitation and emission characteristics ^b		Peak assignment based on this study ^c
Peaks based	on excitation spec	rtra	_
α' A	Ex _{max} <250 nm	λ_{ob} =445 nm	A' (248/461)
α''_{A}	$Ex_{max} \approx 340 \text{ nm}$	$\lambda_{\rm ob}$ =445 nm	C (360/460)
β' _A	Ex _{max} <250 nm	$\lambda_{\rm ob}$ =445 nm	A (239/429)
β″ Α	$Ex_{max} \approx 370 \text{ nm}$	$\lambda_{\rm ob}$ =445 nm	M (328/422)

Peaks based on emission spectra

The values in parentheses are the average Ex_{max} and Em_{max} values for these peaks from Table 1 (also see Fig. 1).

^a From De Souza Sierra et al. (1994). Note that α and β are the symbols of the two proposed sets of chromophores, the single and double prime superscripts represent the two main absorption bands for these proposed chromophores, and the subscript "F" represents the emission (fluorescence) of the proposed chromophores with $\lambda_{\rm ex}$ =370 nm. Also note that with $\lambda_{\rm ex}$ =370 nm it is impossible to observe the fluorescence of peaks $\alpha'_{\rm A}$ (A') or $\alpha''_{\rm A}$ (A).

^b The values of λ_{ex} and λ_{ob} are the excitation and observation (emission) wavelengths used by De Souza Sierra et al. (1994) in determining excitation and emission spectra of their samples. Em_{max} and Ex_{max} are the emission and excitation wavelengths of maximum fluorescence, respectively, for the α and β chromophores, based on these emission and excitation spectra.

 c The values in parentheses are the average Ex_{max} and Em_{max} values for these peaks from Table 1 (also see Fig. 1).

De Souza Sierra et al. (1994). Nevertheless, the ability to make this analogy between our fluorescence data and two proposed chromophore classes in this model provides important evidence in support of our suggestion that the four humic-like peaks we observed in our samples may indeed be paired together as we have described here.

At the same time, results presented in Boehme and Coble (2000) also appear to be consistent with our suggestion of this pairing of humic-like peaks. Starting with riverine and estuarine waters that showed broad peak A and M fluorescence² they used high

energy laser fragmentation (HELF) to show that the spectra of these samples were composed of at least eight more specific (though still unidentified) fluorophore groups. Interestingly, many of the fluorophore groups they detected existed as pairs of peaks with near identical $\rm Em_{max}$ values and different $\rm Ex_{max}$ values. In these peak pairs one peak was always excited by high energy UV light (λ_{ex} < 280 nm) and the other by lower energy UV light (λ_{ex} between ~300 and 380 nm).

An examination of the $\rm Ex_{max}$ and $\rm Em_{max}$ values of all of the peaks observed by Boehme and Coble (2000) indicates that the $\rm Ex_{max}$ values of these high energy UV peaks are roughly in the range of our peaks A and A'. Similarly the low energy UV peaks are in the range of our peaks M and C. Finally, the ~ 60 nm range in $\rm Em_{max}$ values of these HELF peaks also spans the range observed in our samples. Thus, it is not difficult to see how combinations of these eight peaks could form four distinct humic-like peaks, as we see in our samples. Furthermore, since many of these HELF peaks appear to exist as peak pairs it is also not difficult to envision that combinations of these peaks might roughly behave as peak pairs in apparent emission bands.

Finally, one might ask why these pairs of four humic-like peaks have not been observed in previous 3-d fluorescence studies of marine DOM. Although past worker have observed peaks A, M and C (e.g., Coble, 1996; Coble et al., 1998; Del Castillo et al., 1999; Parlanti et al., 2000), the occurrence of peak A' has not been previously reported. We believe that there are at least three possible explanations for this. First, almost all other past studies have examined water column FDOM, where fluorescence intensities are generally lower than those observed here. In such situations, it may be difficult to resolve two distinct, but relatively close peaks (in terms of Ex_{max} and Em_{max} values). Such spectra may therefore simply have what appears to be one broad peak in each region of the spectrum. Second, 3-d fluorescence spectra tend to be quite noisy in the low excitation wavelength region (below ~250 nm) further making it difficult to separately detect and quantify both peaks A and A' at low fluorescence intensities. In contrast, distinct peaks at these low excitation wavelengths may be easier to visualize in 3-d fluorescence spectra of these highly fluorescent pore waters. And third, the use of a long

² Although Boehme and Coble (2000) refer to these peaks as peaks A and C, using the terminology defined in the beginning of this paper we would refer to these peaks as peaks A and M. Furthermore, the appearance of the spectra in this paper suggest to us that these two broad peaks may also tail into peaks A' and C.

pass filter in the emission light path to remove signals from second order Rayleigh and Raman scattering (which was not often used in previous studies) allows for better visualization of fluorescence peaks in the region of peak A'.

4.2. Sources of humic-like fluorescence

Assuming that humic-like fluorescence from these apparent peak pairs (peaks A and M and A' and C) represent fluorescence from different groups of similar fluorophores, we can use this suggestion to further examine the possible sources of these fluorophores. In this discussion we will build on past results that have primarily focused on examining the relationship between peaks M and C. Although these studies generally only report the occurrence of peak A in conjunction with either peak M, C, or M and C, we will assume here that the apparent absence of peak A' is a result of the analytical difficulties outlined above.

Some evidence to date suggests that peak M may be of marine origin (see discussions most recently in Coble et al., 1998) although analyses we have carried out of pore waters from glacial Lake Agassiz peatlands (Burdige et al., 1999a; Chasar et al., 2000) indicates that this peak is observed in this freshwater system. The origin of peak C is also not well constrained. Coble et al. (1993) suggest that peak C is of terrestrial origin, and studies by Parlanti et al. (2000) in the Bay of Frenaye, France, support this suggestion. In this study peak C is only observed in freshwater (riverine) samples, while marine samples contain both peaks M and C. However studies in the Arabian Sea by Coble et al. (1998) suggest that here peak C does not originate from riverine inputs. These observations are consistent with other suggestions (Coble, 1996) that peak M is a blue-shifted version of peak C, implying that the fluorophore(s) responsible for peak C fluorescence is a diagenetically altered form of that responsible for peak M. Such observations are consistent with macro-algae degradation experiments (Parlanti et al., 2000) in which the transient production of both protein-like and peak M fluorescence was initially observed in these experiments, followed by the eventual decline of both of these types of fluorescence and the net accumulation of peak C fluorescence.

Finally, in examining the sources of peaks M and C we consider recent work by McKnight et al. (2001), who observed that the ratio of the fluorescence emission intensity at 450 nm to that at 500 nm (with excitation at 370 nm) serves as an index that distinguishes between autochthonous fulvic acids (in their study microbially derived fulvic acids from Antarctic dry valley lakes) versus those that are allocthonous in origin (e.g., terrestrially derived Suwanee River fulvic acids). With this approach, fluorescence index (FI) values of ~ 1.9 are indicative of these autochthonous sources, while values of 1.4-1.5 are indicative of allocthonous sources. There is also a non-linear inverse relationship between FI and % Aromaticity, with end-member autochthonous fulvic acids (FI=1.7-19) having lower aromaticities than allocthonous fulvic acids (FI=1.3-1.4). In the context of this discussion, if we look at the FI in terms of the 3-d fluorescence spectra we have observed (i.e., see Fig. 1), we see that the 370 nm excitation line cuts across the upper parts of peaks M and C. Therefore, higher values of FI imply a larger relative importance of peak M versus peak C fluorescence.

Putting all of this information together, we suggest that rather than strictly focusing on questions of marine versus terrestrial sources of the fluorophores responsible for humic-like fluorescence peaks, a more unifying approach that incorporates all of the results discussed above addresses this question in terms of the diagenetic state of these fluorophores. In this formalism then, we consider the fluorophores responsible for peak M as being relatively "fresh" and those responsible for peak C as being more diagenetically altered. Thus peak M fluorophores would result from the remineralization of relatively fresh particulate organic matter (as suggested by Coble et al., 1998), and peak C fluorophores from either less reactive particulate organic matter or through diagenetic alteration of DOM or other FDOM intermediates of organic matter remineralization. In this conceptual model, it is important to note that the peak C fluorophores produced by these two different pathways are not necessarily identical. Rather, it simply implies that their fluorescence properties are sufficiently similar that they lead to similar types of fluorescence.

In the absence of additional information about these humic-like fluorophores and the processes affecting their diagenetic cycling it is difficult to examine this model in further detail. However, we believe that in a qualitative sense the model explains much of the above-discussed data (both ours and that in the literature). At the same time though, further work is needed to critically examine its validity (i.e., while the model appears to be consistent with these data, it also may not actually be the correct explanation of these results). Similarly, while the discussion in Section 4.1 regarding the pairing of humic-like fluorescence peaks is consistent with the data presented here (both in our work and in the studies cited above), more work is again needed to identify the specific fluorophores responsible for this fluorescence.

Regardless of any diagenetic relationship between peaks M and C (or peaks A and A'), the A'/C peak pair is red-shifted (occurs at longer wavelengths), most strongly in emission wavelengths, relative to the A/M pair. A red shift in fluorescence emission is caused by a decrease in the energy difference between the ground state and the first excited state of a molecule. This may result from structural changes in a fluorescent molecule that increase the extent of its π electron system. Examples of this include an increase in the number of aromatic rings, an increase of conjugated bonds in a chain structure, or the conversion of a linear ring system to a nonlinear system (Berlman, 1971; Senesi, 1990). Similarly, the addition of certain functional groups (such as carbonyl, hydroxyl and amino groups) can also lead to fluorescence red shifts (Murrel, 1963; Senesi, 1990).

In light of this observation, the possibility then exists that in situ transformations could lead to peak A and M fluorophores being altered to peak A' and C fluorophores (e.g., Coble et al., 1998). Such processes are, for example, consistent with both classical views of humification (Hedges, 1988) as well as general observations in the literature that degradation and/or "aging" of organic matter leads to progressive red shifts in Exmax and Emmax values (see Komada et al., 2002, and references therein). At the same time though, terrestrial organic matter is generally rich in aromatic components (e.g., from the occurrence of lignocellulose in vascular plant materials; Hedges et al., 1988), consistent with the possibility of the direct production of peak A' and C fluorophores from this material. Since the fluorescence observed for these peaks almost certainly results from multiple fluorophores, it is also not unrealistic to consider the possibility that the production of peak A'/C fluorophores occurs by both mechanisms.

Finally, we can briefly examine this conceptual model in the context of past general observations that terrestrial FDOM excitation and emission spectra are red-shifted relative to those for marine FDOM (e.g., Donard et al., 1989; De Souza Sierra et al., 1994, 1997; Coble, 1996). Similar spectral shifts presumably lead to a decrease in the McKnight et al. (2001) fluorescence index, which they interpret as resulting from a greater proportion of allocthonous (terrestrial) versus autochthonous (microbial) fulvic acids. However as discussed above, many of these observations are based on single wavelength excitation or emission scans as opposed to 3-d fluorescence scans. With this former approach we believe that it is difficult to differentiate between production of independent sets of fluorophores (from, e.g., marine versus terrestrial organic matter) versus diagenetic alteration of a single set of fluorophores. Thus, the model presented here is not inconsistent with these observations.

4.3. Pore water fluorescence and its relationship to models of sediment DOC cycling

In this section we will examine the relationship between pore water DOM fluorescence and a conceptual model for pore water DOM cycling in marine sediments, the pore water DOM size/reactivity (PWSR; Burdige and Gardner, 1998). Additional details about the model can be found in Burdige (2002) along with the presentation of a quantitative advection/diffusion/reaction model for pore water DOM dynamics based on the PWSR model. The discussion in this section will focus on examining humic-like fluorescence in the context of the PWSR model, while the relationship between protein-like fluorescence and the PWSR model will be discussed in Section 4.7 after a more complete discussion of our benthic flux results.

In the PWSR model the remineralization of sediment organic matter (SOM) to inorganic nutrients is proposed to occur through the production and consumption of DOM intermediates of increasingly smaller molecular weights. The model assumes that the initial hydrolysis or depolymerization of SOM produces a class of reactive high molecular weight

DOM compounds (HMW-DOM) that contains materials such as dissolved proteins and polysaccharides. Along with the remineralization of the HMW-DOM to inorganic nutrients there is also proposed to be some small net production of refractory, relatively low molecular weight DOM, referred to in this model as polymeric low molecular weight DOM, or pLMW-DOM. This pLMW-DOM is presumed to be much less reactive than other high and low molecular weight DOM intermediates produced and consumed during SOM remineralization. This then leads to an imbalance between sediment DOM production and consumption, and to a first order, the accumulation of refractory low, and not high, molecular weight DOM with depth in sediment pore waters. These observations about pLMW-DOM production are consistent with recent thoughts about humification, in which it is now thought that the production of dissolved humic substances initially occurs via the production of increasingly oxidized, low molecular weight DOM molecules from particulate organic matter (Hatcher and Spiker, 1988; Amon and Benner, 1996; also see earlier discussions in Waksman, 1938).

Looking at our fluorescence data in the context of the PWSR model we see that humic-like fluorescence generally increased with sediment depth, and was closely coupled with total DOC concentrations (Fig. 5) in a way that is similar to that observed by other workers (Chen et al., 1993; Skoog et al., 1996; Sierra et al., 2001; Komada et al., 2002). Based on this discussion we therefore propose that humic-like fluorescence represents a tracer for this relatively low molecular weight refractory pLMW-DOM produced during SOM diagenesis/remineralization that represents the majority of the DOC (and DON) in marine sediment pore waters.

4.4. Fluorescence of pore water DOM—comparison of sites

Pore water DOC concentrations and humic-like fluorescence were tightly coupled in these sediments (e.g., see Fig. 5 and Table 3), as has been observed previously in other marine sediments (see references above). Pore water humic fluorescence and DOC and DON concentrations were also all much higher at sta. M3 than in the other Chesapeake Bay site (sta. S3) and in the MASSB sediments. Higher inputs of

organic matter to sta. M3 sediments and a greater degree of sediment anoxia both likely play a role here (Burdige and Zheng, 1998; Burdige, 2001). The near-constant depth profiles of humic-like fluorescence at sta. S3 (Fig. 2) are consistent with DOC and DON profiles at this site which show little seasonal or depth variability in the upper ~20 cm of sediment (Burdige, 2001). This is likely related to the extensive bioturbation and bioirrigation of these sediments, and associated changes in sediment redox conditions (also see Burdige, 2002 and Section 4.5 for further details).

In light of the discussions above, it is perhaps surprising that the peak M/peak C ratio showed such constancy both with depth at any given site and among the different sites (Table 2). In recent work by Sierra et al. (2001) using single wavelength emission scans of sediment pore waters (λ_{ex} =313 nm) they observed an emission blue shift in surface sediment pore waters (0-2 cm) as they moved out into the Gulf of Biscay (France) from water depths between 400 and 3040 m. Such blue shifts were interpreted by these workers as implying that as one moves offshore there is a greater input of marine (vs. terrestrial) organic matter to the sediments, contributing to an increasing marine fluorescence signature of the surface sediment pore waters. They also observed a red shift in fluorescence emission with depth in many of these cores (upper 30 cm). As discussed in Section 4.2 these red shifts could either be interpreted as being indicative of the importance of less reactive terrestrial organic material undergoing remineralization at depth, or of diagenetic transformations of marine-derived fluorophores (e.g., transformation of peaks A/M fluorophores to peaks A'/C fluorophores).

Using the conceptual model in Section 4.2 to explain the constant peak M/peak C ratio seen in our sediment pore waters leads to two possible explanations. The first is that marine and terrestrial (autochthonous and allocthonous) sources are both responsible for the production of humic-like fluorophores, and that their production and consumption are both balanced in such a way as to lead to this constant fluorescence ratio. Alternately, there may be only a single initial source of these fluorophores and diagenetic transformations lead to the production of both classes of fluorophores.

Unfortunately, attempts to distinguish between these two interpretations using other data from these sediments yields contradictory results. While the fluorescence peaks observed here are consistent with the possible occurrence of both autochthonous and allocthonous sources, the McKnight et al. (2001) FI index for these pore waters is more similar to an autochthonous rather than allocthonous end-member (Burdige and Hu, unpublished data). Furthermore, organic matter at all of these sites appears to be largely marine-derived, based on a limited number of δ^{13} C analyses of the SOM at sta. M3, S3 and WC7 (approximately -21% to -22%J. Cornwell, unpublished isotope data cited in Marvin-DiPasquale and Capone, 1998; Burdige, unpublished data). However, in these Chesapeake Bay sediments and at other sites along the mid-Atlantic shelf/slope break there is also evidence for the occurrence of some terrestrially derived organic matter in the bulk SOM pool and/or in the SOM undergoing remineralization (Burdige, 1991; Harvey, 1994). Finally, pore water DOC and DON data from these sites suggests that terrestrial sources could be important sources of this DOM, since the C/N ratios of the pore water DOM in these sediments are generally greater than the value of 6.6 for marine, Redfield-like organic matter (Burdige and Zheng, 1998; Burdige, 2002).

In the absence of further information about the pathways of sediment organic matter remineralization, it is difficult to more critically discuss these observations in any further detail. More information is clearly needed on the relationship between FDOM cycling and overall pathways of sediment organic matter remineralization and the production of refractory DOM in sediment pore waters to further examine these observations.

4.5. Fluorescence-DOC relationships

The observation that the fluorescence of the four humic-like peaks is strongly correlated with DOC concentrations (Fig. 5 and Table 3) is not surprising, based on the results of past studies (Chen et al., 1993; Skoog et al., 1996; Seretti et al., 1997; Sierra et al., 2001). What is perhaps more interesting about the observations in Fig. 5 is that different slopes were observed for these DOC-fluorescence relationships in estuarine versus shelf/slope break sediments. Given the apparent similarities in the humic-like fluorophores found in these sediments, the simplest

explanation for these different slopes is that there is greater dilution of FDOM in the total DOC pool in shelf/slope break sediments than there is in estuarine sediments.

In further examining these observations we note that Komada et al., (2004) observed similar differences for humic-like fluorescence that roughly corresponds to peak M in the fluorescence-DOC relationship for nearshore anoxic versus oxic/sub-oxic sediments. However, in contrast to our results they observed slopes for these contrasting sites that differed by only $\sim 25\%$ (versus the factor of >4 differences seen here). In light then of these observations, we suggest that these differences in DOC-fluorescence relationships are likely controlled by sediment redox conditions, with larger relative amounts of humic-like FDOM seen in anoxic sediments (i.e., the sta. M3 sediments) versus that observed in sub-oxic or mixed redox sediments (i.e., the sta. S3 and MASSB sediments). This suggestion then builds on the observation discussed in Section 3.3 which suggests that the sta. S3 DOC-normalized fluorescence values are actually more similar to MASSB values than they are to sta. M3 values (e.g., see Figs. 4 and 5).

By extension, these observations also suggest that refractory humic-like compounds (in general) are preferentially preserved in sediment pore waters under anoxic conditions. Independent evidence in support of this idea comes from calculations initially presented in Burdige (2001), in which uncharacterized pore water DOC ([DOC]_{unc}) was estimated with pore water DOC, DON and dissolved carbohydrate data. These calculations indicated that [DOC]_{unc} was a higher percentage of the total DOC in the anoxic sta. M3 sediments ($\sim 70\%$) than it was in the mixed redox sediments at sta. S3 (~45%). Similar calculations carried out for the MASSB sediments (using unpublished DON data, and DOC and carbohydrate data presented in Burdige et al., 2000) yields percentages of [DOC]_{unc} in MASSB sediments (~40%) that are similar to that observed at sta. S3.

As discussed in Burdige (2001) this [DOC]_{unc} may represent dissolved humic substances that are apparently preferentially preserved under anoxic conditions. This suggestion was further explored in Burdige (2002) using an advection/diffusion/reaction pore water model for DOC in marine sediments that explicitly incorporates bioturbation, bioirrigation and

enhanced remineralization of humic-like pore water DOC under mixed redox (and oxic/sub-oxic) sedimentary conditions (also see similar modeling results in Komada et al., 2004). All of these results (including the DOC-normalized fluorescence values presented here in Figs. 4 and 5) are consistent with this assumption that sediment redox conditions alter the pathways of DOM remineralization, and lead to higher concentrations of refractory humic-like DOM in anoxic sediments. As discussed in Burdige (2001, 2002) this suggestion also has implications for how DOM cycling and sediment redox conditions may affect sediment carbon burial and preservation.

4.6. Benthic fluxes of FDOM

At sta. M3 there was good agreement between measured and calculated, diffusive DOC and FDOM benthic fluxes (Table 4 and Fig. 7), as has been observed in other benthic flux studies at this site (see Burdige, 2001, for a summary). Such observations imply that diffusion is the dominant transport process for dissolved constituents across the sediment—water interface at this site. Consistent with this, the DOC-normalized fluxes of humic-like fluorophores at sta. M3 were similar to the corresponding fluorescence/DOC ratios in the pore waters at this site (compare Tables 3 and 4).

At sta. S3 measured benthic fluxes of both total DOC and humic-like FDOM were significantly larger than calculated, diffusive fluxes, presumably due to the bioturbation and bioirrigation of these sediments (e.g., Burdige, 2001). The similarity of values of *R* at sta. S3 for DOC and humic-like fluorophores (Fig. 7) is also consistent with discussions in Section 4.3 in which we suggested that humic-like fluorescence is a tracer for the relatively refractory pLMW-DOM.

In contrast though, measured and calculated, diffusive fluxes of protein-like FDOM were more similar to one another at sta. S3. Possible explanations for this observation comes from modeling results presented in Burdige (2002) which were used to examine sediment DOM cycling in mixed redox sediments such as those at sta. S3. These model results indicate that the net production of reactive, HMW-DOM is concentrated in the upper ~ 1 cm of sediment while net production of refractory, pLMW-DOM extends to depths >4 cm.

Furthermore, because rates of HMW-DOM cycling near the sediment—water interface are rapid relative to typical rates of bioturbation or bioirrigation, these macrofaunal processes have minimal effects on depth profiles of reactive DOM intermediates. Therefore pore water profiles of reactive HMW-DOM are much less affected by the occurrence of either bioturbation or bioirrigation than are pore water profiles for total DOM (≈ refractory pLMW-DOM). This then leads to differences in the effects of bioirrigation on both pore water profiles for different DOM fractions as well as their benthic fluxes.

These observations therefore suggest that at least for benthic fluxes, protein-like fluorescence may trace reactive DOM intermediates of sediment organic matter remineralization (such as dissolved proteins and peptides) that are produced near the sedimentwater surface and (some of which) escape the sediments as a benthic flux (see related discussions in Burdige, 2002). Thinking about this in the context of the controls on benthic FDOM fluxes, we also see the effects here of the interplay between transport processes and the depth zonation of DOM cycling. For humic-like fluorescence (and therefore refractory pLMW-DOM and most DOC in general) bioirrigation dominates sediment-water exchange of this material at sites such as sta. S3, as might be expected. In contrast though, molecular diffusion plays a much more important role in controlling the benthic flux of the much smaller sub-set of the total DOM pool responsible for protein-like fluorescence.

Interestingly, these observations are also consistent with discussions in Aller (2001) regarding the relationship between benthic fluxes, bioirrigation and the depth-distribution of sediment processes. Based on the results of studies of inorganic pore water solutes and their sediment-water exchange, he notes that bioirrigation has differing effects on benthic fluxes of pore water solutes whose reactivity occurs close to the sediment-water interface (i.e., here protein-like fluorescence or HMW-DOM), versus those whose production occurs "deeper" in the sediments (i.e., here humic-like fluorescence or pLMW-DOM). Furthermore, based on the discussion in Aller (2001), R values for either total DOC or humic-like fluorescence would also be expected to be larger than those for protein-like fluorescence, as is observed in Fig. 7.

4.7. Protein-like fluorescence revisited

When compared with model calculations in Burdige (2002) the results of benthic flux studies in (Fig. 7) are consistent with the suggestion that protein-like fluorescence near the sediment—water interface results from reactive DOM intermediates of SOM remineralization. However the same may not be the case for protein-like fluorescence in sediment pore waters.

Protein-like fluorescence in these sediment pore waters co-varied with total DOC concentrations (Fig. 6) in a manner similar to that seen for humic-like fluorescence. This suggests that in sediment pore waters protein-like fluorescence might be more associated with refractory pLMW-DOM. At the same time though, spectral interferences with the broad humiclike peaks (Mayer et al., 1999) could also play a role in explaining the observations in Fig. 6, because of the tight coupling between DOC and humic-like fluorescence. However discussions and model calculations in Burdige (2002) indicate that reactive DOM intermediates in sediments pore waters are generally less than a few percent of the total DOC, except just below the sediment surface. Thus if protein-like fluorescence in pore waters results from reactive DOM intermediates then it should be masked (overwhelmed) by the more intense humic-like fluorescence associated with the bulk of the pore water DOM.

Therefore these observations suggest that the fluorophores responsible for protein-like fluorescence may occur in both reactive and refractory DOM intermediates and that their relative importance differs in sediment pore water DOM versus that which escapes the sediments as a benthic flux. This "uncoupling" of the linkage between protein-like fluorescence and DOM pools with widely different degrees of reactivity is not necessarily surprising, and is in fact consistent with conclusions reached in Burdige (2001) for the DOM pool in general, based solely on bulk DOC and DON pore water concentrations and benthic fluxes. Additional work is however needed to better resolve the source(s) of protein-like fluorescence in natural systems to more definitively interpret these fluorescence signals in terms of organic matter diagenesis and DOM cycling. At the same time, better discrimination between peaks associated with tryptophan and tyrosine fluorescence would also aid in addressing this problem, based in part on suggestions in Mayer et al. (1999) that the tyrosine:trypotophan intensity ratio might be a useful indicator of the degradative state of dissolved proteins and peptides.

4.8. Sediments as sources of FDOM to coastal water

The presence of colored and fluorescent DOM (CFDOM) in the water column significantly affects the optical and photochemical properties of marine waters. Past studies have identified riverine transport (e.g., Blough et al., 1993) and phytoplankton degradation products (e.g., Carder et al., 1991; Rochelle-Newall and Fisher, 2002) as sources of CFDOM to the water column. The results of our study further suggest that sediments represent an additional source of CFDOM to the water column (also see Fox, 1991; Mayer et al., 1999; Boss et al., 2001).

Table 6
The impact of sediment-derived FDOM on water column FDOM pools

Pools			
Station/peak	Flux	Average water	% water column
	$(\mu g \ QS \ m^{-2})$	column conc.	FDOM derived
	day ⁻¹) ^a	(ppb QS) ^b	from sediments ^c
Station M3			
peak A	314	28	25 - 33%
peak M	166	16	24-32%
peak A'	328	25	29-39%
peak C	171	12	32-43%
Station S3			
peak A	62	25	6 - 8%
peak M	43	12	8 - 11%
peak A'	55	21	6-8%
peak C	45	9	11-14%
Average value	es		
peak A			15-20%
peak M			16-21%
peak A'			17 - 23%
peak C			21-29%

^a From Table 4.

^b Based on water column samples collected during cruises CH XVII, XIX and XX.

^c Assuming a water residence time in the Bay of 9-12 months (Skrabal et al., 1997), the concentration of FDOM (F) added to the Bay during this time period is given by $F=B\tau/h$, where B is the benthic flux, τ is the water residence time and h is the average depth of the Bay (=12 m). The ratio of F to the average water column concentration at each site then yields the percentages shown here.

Past work examining benthic fluxes of total DOC have shown that these fluxes are small in comparison to oceanic DOC recycling rates (e.g., Chen et al., 1993), although integrated DOC fluxes from estuarine, coastal and continental margin sediments are significant in comparison to net sources of DOC to the oceans such as riverine DOC transport (see most recently Burdige et al., 1999b). Thus, in such regions where riverine inputs of CFDOM likely have their greatest impact on water column optical properties, benthic fluxes of CFDOM should also be of importance as compared to riverine CFDOM sources. Furthermore, pore water DOM is enriched in chromophoric material as compared to water column DOM (Fig. 4; also see Chen et al., 1994), and the importance of benthic fluxes of CFDOM may accordingly be increased as compared to riverine sources of this material.

To examine this problem more quantitatively for the Chesapeake Bay, we have used the approach described in Skrabal et al. (1997) to estimate the fraction of water column fluorescence that could be derived from sediments as a result of the benthic fluxes reported in Table 4. The results of these calculations are shown in Table 6, and indicate that benthic fluxes could supply $\sim 15-30\%$ of the FDOM in Chesapeake Bay waters. While more detailed studies will be needed to further quantify all of these processes that affect the cycling of CFDOM in the marine environments, this simple calculation points to the importance of sediment CFDOM sources in some marine settings.

5. Summary and conclusions

- 1. The major fluorescence peaks observed in pore waters from sites in the Chesapeake Bay and along the mid-Atlantic shelf/slope break were similar to those observed in the water column. These included peaks ascribed to the fluorescence of humic-like material (peaks A, C and M), as well as protein-like peaks that appear to result from the fluorescence of the aromatic amino acids tryptophan and tyrosine.
- 2. In these pore waters we also observed a fourth humic-like fluorescence peak (A'). These four humic-like peaks appeared to occur as pairs of

- peaks (peaks A and M in one pair and peaks A' and C in a second pair) with near identical $\rm Em_{max}$ values but different $\rm Ex_{max}$ values for each pair. Peaks A' and C was red shifted relative to the peaks A and M.
- 3. Humic-like fluorescence generally increased with sediment depth, and was closely correlated with pore water total DOC concentrations. This fluorescence appeared to represent a tracer for the refractory, relatively low molecular weight pore water DOM that accumulates with depth during sediment organic matter diagenesis.
- 4. Fluorescence—DOC relationships indicated that larger relative amounts of humic-like FDOM were seen in anoxic sediments (i.e., the sta. M3 sediments) than in sub-oxic or mixed redox sediments (i.e., the sta. S3 and MASSB sediments). By extension, these observations suggest that refractory humic-like compounds (in general) are preferentially preserved in sediment pore waters under anoxic conditions.
- 5. Protein-like fluorescence showed no coherent depth trends in sediment pore waters, other than the fact that pore water fluorescence intensities were greater than bottom water values. Based on the results of benthic flux studies, it appeared that protein-like fluorescence was associated with reactive DOM intermediates of organic matter diagenesis (e.g., dissolved peptides and proteins) produced near the sediment—water interface. In contrast, in sediment pore waters protein-like fluorescence may be associated with amino acids (peptides?) incorporated into refractory, humic-like structures, although this suggestion will require further verificiation.
- 6. Based on a simple conceptual model for FDOM cycling, structural differences in FDOM that lead to red shifts in peak A'/C fluorophores (relative to the peak A/M fluorophores) may be the result of several processes. These include in situ transformations producing peaks A'/C fluorophores from peaks A/M fluorophores, as well as direct production of peak A'/C fluorophores from terrestrial organic matter.
- 7. In bioirrigated sediments the interplay between transport processes and the depth zonation of DOM cycling leads to a situation in which molecular diffusion (rather than bioirrigation) plays a much

- more important role in transporting protein-like fluorescence (i.e., reactive HMW-DOM) out of these sediments. In contrast, bioirrigation dominates sediment—water exchange of humic-like fluorescence (and therefore more refractory pLMW-DOM and most DOC in general) in such sediments.
- 8. Benthic flux studies indicated that sediments represent a source of chromophoric DOM to coastal waters, although further work will be needed to quantify their significance in terms of other known sources (e.g., riverine input, phytoplankton degradation products).

Acknowledgements

This work was supported by the Office of Naval Research Environmental Optics Program (CoBOP DRI). Ship-time support was provided by a grant to DJB and J. Donat from the ONR Harbor Processes Program. We thank Kip Gardner for his assistance with several aspects of this work, Carlos del Castillo for all of his help throughout this work, and two anonymous reviewers and Paula Coble for insightful comments on earlier versions of this manuscript.

References

- Aller, R.C., 1994. Bioturbation and remineralization of sedimentary organic matter: effects of redox oscillation. Chem. Geol. 114, 331–345.
- Aller, R.C., 2001. Transport and reactions in the bioirrigated zone. In: Boudreau, B.P., Jørgensen, B.B. (Eds.), The Benthic Boundary Layer. Oxford Univ. Press, Oxford, pp. 269–301.
- Alperin, M.J., Albert, D.B., Martens, C.S., 1994. Seasonal variations in production and consumption rates of dissolved organic carbon in an organic-rich coastal sediment. Geochim. Cosmochim. Acta 58, 4909–4929.
- Alperin, M.J., Martens, C.S., Albert, D.B., Suayah, I.B., Benninger, L.K., Blair, N.E., Jahnke, R.A., 1999. Benthic fluxes and porewater concentration profiles of dissolved organic carbon in sediments from the North Carolina continental slope. Geochim. Cosmochim. Acta 63, 427–448.
- Amon, R.M.W., Benner, R., 1996. Bacterial utilization of different size classes of dissolved organic matter. Limnol. Oceanogr. 41, 41–45.
- Benamou, C., Richou, M., Benaim, J.Y., Loussert, A., Bartholin, F., Richou, J., 1994. Laser-induced fluorescence of marine

- sedimentary interstitial dissolved organic matter. Mar. Chem. 46, 7–23.
- Berlman, I.B., 1971. Handbook of Fluorescence Spectra of Aromatic Molecules. Academic Press, New York. 258 pp.
- Blough, N.V., Green, S.A., 1995. Spectroscopic characterization and remote sensing of nonliving organic matter. In: Zepp, R.G., Sonntag, C. (Eds.), Role of Non-Living Organic Matter in the Earth's Carbon Cycle. Wiley, Chichester, pp. 23–45.
- Blough, N.V., Zafiriou, O.C., Bonilla, J., 1993. Optical absorption spectra of waters from the Orinoco River outflow: terrestrial input of colored dissolved organic matter to the Caribbean. J. Geophys. Res. 98, 22718.
- Boehme, J.R., Coble, P.G., 2000. Characterization of colored dissolved organic matter using high-energy laser fragmentation. Environ. Sci. Technol. 34, 3283–3290.
- Boss, E., Pegau, W.S., Zaneveld, J.R.V., Barnard, A.H., 2001. Spatial and temporal variability of absorption by dissolved material at a continental shelf. J. Geophys. Res. 106, 9499–9507.
- Burdige, D.J., 1991. The kinetics of organic matter mineralization in anoxic marine sediments. J. Mar. Res. 49, 727–761.
- Burdige, D.J., 2001. Dissolved organic matter in Chesapeake Bay sediment pore waters. In: Canuel, E., Bianchi, T. (Eds.), Organic Geochemical Tracers in Estuaries. Org. Geochem., vol. 32, pp. 487–505.
- Burdige, D.J., 2002. Sediment pore waters. In: Hansell, D.A., Carlson, C.D. (Eds.), Biogeochemistry of Marine Dissolved Organic Matter Academic Press, San Diego, pp. 612–664.
- Burdige, D.J., Gardner, K.G., 1998. Molecular weight distribution of dissolved organic carbon in marine sediment pore waters. Mar. Chem. 62, 45-64.
- Burdige, D.J., Zheng, S., 1998. The biogeochemical cycling of dissolved organic nitrogen in estuarine sediments. Limnol. Oceanogr. 43, 1796–1813.
- Burdige, D.J., Alperin, M.J., Homstead, J., Martens, C.S., 1992. The role of benthic fluxes of dissolved organic carbon in oceanic and sedimentary carbon cycling. Geophys. Res. Lett. 19, 1851–1854.
- Burdige, D.J., Kline, S.W., Chasar, L.S., Chanton, J.P., Glaser, P., Siegel, D.I., 1999a. Examination of dissolved organic matter (DOM) sources using fluorescence spectroscopy. EOS 80 (49), OS21K-02 (abstr.).
- Burdige, D.J., Berelson, W.M., Coale, K.H., McManus, J., Johnson, K.S., 1999b. Fluxes of dissolved organic carbon from California continental margin sediments. Geochim. Cosmochim. Acta 63, 1507–1515.
- Burdige, D.J., Skoog, A., Gardner, K.G., 2000. Dissolved and particulate carbohydrates in contrasting marine sediments. Geochim. Cosmochim. Acta 64, 1029–1041.
- Carder, K.L., Hawes, S.K., Baker, K.A., Smith, R.C., Stewart, R.G., Mitchell, B.G., 1991. Reflectance model for quantifying chlorophyll a in the presence of productivity degradation products. J. Geophys. Res. 96 (20) (1991) 599–520,611.
- Chasar, L.S., Chanton, J.P., Glaser, P.H., Siegel, D.I., Rivers, J.S., 2000. Radiocarbon and stable carbon isotopic evidence for transport and assimilation of dissolved organic carbon, dissolved inorganic carbon and CH4, in a northern Minnesota peatland. Glob. Biogeochem. Cycles 14, 1095–1108.

- Chen, R.F., Bada, J.L., 1989. Seawater and porewater fluorescence in the Santa Barbara Basin. Geophys. Res. Lett. 16, 687–690.
- Chen, R.F., Bada, J.L., 1994. The fluorescence of dissolved organic carbon in porewaters of marine sediments. Mar. Chem. 45, 31–42.
- Chen, R.F., Bada, J.L., Suzuki, Y., 1993. The relationship between dissolved organic carbon (DOC) and fluorescence in anoxic marine porewaters: implications for estimating benthic DOC fluxes. Geochim. Cosmochim. Acta 57, 2149–2153.
- Coble, P.G., 1996. Characterization of marine and terrestrial DOM in seawater using excitation-emission matrix spectroscopy. Mar. Chem. 51, 325-346.
- Coble, P.G., Green, S., Blough, N.V., Gagosian, R.B., 1990. Characterization of dissolved organic matter in the Black Sea by fluorescence spectroscopy. Nature 348, 432–435.
- Coble, P.G., Mopper, K., Schultz, C.S., 1993. Fluorescence contouring analysis of DOC intercalibration experiment samples: a comparison of techniques. Mar. Chem. 41, 173–178.
- Coble, P.G., Del Castillo, C.E., Avril, B., 1998. Distribution and optical properties of CDOM in the Arabian Sea during the 1995 southwest monsoon. Deep-Sea Res. 45, 2195–2223.
- Del Castillo, C.E., Coble, P.G., Morell, J.M., Lopez, J.M., Corredor, J.E., 1999. Analysis of the optical properties of the Orinoco River plume by absorption and fluorescence spectroscopy. Mar. Chem. 66, 35–51.
- De Souza Sierra, M.M., Donard, O.X.F., Lamotte, M., Belin, C., Ewald, M., 1994. Fluorescence spectroscopy of coastal and marine waters. Mar. Chem. 47, 127–144.
- De Souza Sierra, M.M., Donard, O.F.X., Lamotte, M., 1997. Spectral identification and behavior of dissolved organic fluorescent material during estuarine mixing. Mar. Chem. 58, 51–58.
- Donard, O.F.X., Lamotte, M., Belin, C., Ewald, M., 1989. Highsensitivity fluorescence spectroscopy of Mediterranean waters using a conventional or pulsed laser excitation source. Mar. Chem. 27, 117–136.
- Ferdelman, T.A., 1994. Oceanographic and geochemical controls on sulfur diagenesis in coastal sediments. PhD Thesis, Univ. of Delaware.
- Fox, L.E., 1991. The transport and composition of humic substances in estuaries. In: Baker, R.A. (Ed.), Organic Substances and Sediments in Water. Humics and Soils, vol. 1. Lewis Pub., Chelsea, pp. 129–162.
- Green, S.A., Blough, N.V., 1994. Optical absorption and fluorescence properties of chromophoric dissolved organic matter in natural waters. Limnol. Oceanogr. 39, 1903–1916.
- Harris, D.A., Bashford, C.L., 1987. Spectrophotometry and Spectrofluorimetry: A Practical Approach. IRL Press, Washington, DC. 176 pp.
- Harvey, H.R., 1994. Fatty acids and sterols as source markers of organic matter in sediments of the North Carolina continental slope. Deep-Sea Res. 41, 783-796.
- Hatcher, P.G., Spiker, E.C., 1988. Selective degradation of plant biomolecules. In: Frimmel, F.C., Christman, R.C. (Eds.), Humic Substances and Their Role in the Environment. Wiley, Chichester, pp. 59–74.
- Hedges, J.I., 1988. Polymerization of humic substances in natural environments. In: Frimmel, F.C., Christman, R.C. (Eds.), Hu-

- mic Substances and Their Role in the Environment. Wiley, Chichester, pp. 45-58.
- Hedges, J.I., Clark, W.A., Cowie, G.L., 1988. Organic matter sources to the water column and surficial sediments of a marine bay. Limnol. Oceanogr. 33, 1116–1136.
- Holland, J.F., Teets, R.E., Kelly, P.M., Timnick, A., 1977. Correction of right-angle fluorescence measurements for the absorption of excitation radiation. Anal. Chem. 49, 706–710.
- Komada, T., Reimers, C.E., Luther III, G.W., Buckholtz ten Brink, M., Burdige, D.J., 2004. Factors affecting dissolved organic matter dynamics in suboxic to anoxic coastal sediments. Geochim. Cosmochim. Acta, in press.
- Komada, T., Schofield, O.M.E., Reimers, C.E., 2002. Fluorescence characteristics of organic matter released from coastal sediments during resuspension. Mar. Chem. 79, 81–97.
- Lakowicz, J.R., 1999. Principles of Fluorescence Spectroscopy, 2nd ed. Plenum, New York.
- Lyursarev, S.V., Gorshkova, O.N., Chubarov, V.V., 1984. Studies of dissolved colloidal organic matter in marine and interstitial water by laser fluorimetry. Oceanology 24, 71–75.
- Martin, W.R., McCorkle, D.C., 1993. Dissolved organic carbon concentrations in marine pore waters determined by high-temperature oxidation. Limnol. Oceanogr. 38, 1464–1479.
- Matthews, B.J.H., Jones, A.C., Theodorou, N.K., Tudhope, A.W., 1996. Excitation–emission-matrix fluorescence spectroscopy applied to humic bands in coral reefs. Mar. Chem. 55, 317–332.
- Mayer, L.M., Schick, L.L., Loder III, T.C. 1999. Dissolved fluorescence in two Maine estuaries. Mar. Chem. 64, 171–179.
- McKnight, D.M., Boyer, E.W., Westerhoff, P.K., Doran, P.T., Kulbe, T., Andersen, D.T., 2001. Spectrofluorometric characterization of dissolved organic matter for indication of precursor organic material and aromaticity. Limnol. Oceanogr. 46, 38–48.
- Mopper, K., Schultz, C.A., 1993. Fluorescence as a possible tool for studying the nature and water column distribution of DOC components. Mar. Chem. 41, 229–238.
- Mopper, K., Feng, Z., Bentjen, S.B., Chen, R.F., 1996. Effects of cross-flow filtration on absorption and fluorescence properties of seawater. Mar. Chem. 55, 53-74.
- Mopper, K., Sarpal, R.S., Kieber, D.J., 1996. Protein and humic substance fluorescence of dissolved organic matter in Antarctic sea water. Antarc. J. U.S. 30, 137–139.
- Murrel, J.N., 1963. The Theory of the Electronic Spectra of Organic Molecules. Wiley, New York. 328 pp.
- Parlanti, E., Wörz, K., Geoffrey, L., Lamotte, M., 2000. Dissolved organic matter fluorescence spectroscopy as a tool to estimate biological activity in a coastal zone submitted to anthropogenic inputs. Org. Geochem. 31, 1765–1781.
- Rochelle-Newall, E.J., Fisher, T.R., 2002. Production of chromophoric dissolved organic matter fluorescence in marine and estuarine environments: an investigation into the role of phytoplankton. Mar. Chem. 77, 7–21.
- Senesi, N., 1990. Molecular and quantitative aspect of the chemistry of fulvic acid and its interactions with metal ions and organic chemicals: Part II. The fluorescence spectroscopy approach. Anal. Chim. Acta 232, 77–106.
- Seretti, A., Nannicini, L., Del Vecchio, R., Giordani, P., Balboni, V.,

- Ingle, J.D., 1997. Optical properties of sediment pore waters of the Adriatic Sea. Toxicol. Environ. Chem. 61, 195–209.
- Sierra, M.M.D., Donard, O.F.X., Etcheber, H., Soriano-Sierra, E.J., Ewald, M., 2001. Fluorescence and DOC contents of pore waters from coastal and deep-sea sediments in the Gulf of Biscay. Org. Geochem. 32, 1319–1328.
- Skrabal, S.A., Donat, J.R., Burdige, D.J., 1997. Fluxes of coppercomplexing ligands from estuarine sediments. Limnol. Oceanogr. 42, 992–996.
- Skoog, A., Hall, O.J., Hulth, S., Paxeus, N., Van Der Loeff, M.R., Westerlund, S., 1996. Early diagenetic production and sedi-
- ment-water exchange of fluorescent dissolved organic matter in he coastal environment. Geochim. Cosmochim. Acta 60, 3619-3629.
- Tucker, S.A., Amszi, V.L., Acree, W.E.J., 1992. Primary and secondary inner filter effects. J. Chem. Educ. 69, A9-A12.
- Waksman, S.A., 1938. Humus, Origin, Chemical Compositions and Importance in Nature Williams & Wilkins, Baltimore.
- Yappert, M.C., Ingle Jr., J.D. 1989. Correction of polychromatic luminescence signals for inner-filter effects. Appl. Spectrosc. 43, 759–767.